

# PaaS: Planning as a Service for reactive driving in CARLA Leaderboard

Truong Nhat Hao, Mai Huu Thien, Tran Tuan Anh, Tran Minh Quang,  
Nguyen Duc Duy, Pham Ngoc Viet Phuong

**Abstract**—End-to-end deep learning approaches has been proven to be efficient in autonomous driving and robotics. By using deep learning techniques for decision-making, those systems are often referred to as a black box, and the result is driven by data. In this paper, we propose PaaS (Planning as a Service), a vanilla module to generate local trajectory planning for autonomous driving in CARLA simulation. Our method is submitted in International CARLA Autonomous Driving Leaderboard (CADL), which is a platform to evaluate the driving proficiency of autonomous agents in realistic traffic scenarios. Our approach focuses on reactive planning in Frenét frame under complex urban street’s constraints and driver’s comfort. The planner generates a collection of feasible trajectories, leveraging heuristic cost functions with controllable driving style factor to choose the optimal-control path that satisfies safe travelling criteria. PaaS can provide sufficient solutions to handle well under challenging traffic situations in CADL. As the strict evaluation in CADL Map Track, our approach ranked 3rd out of 9 submissions regarding the measure of driving score. However, with the focus on minimizing the risk of maneuver and ensuring passenger safety, our figures corresponding to infraction penalty dominate the two leading submissions by 20%.

**Index Terms**—autonomous driving, dynamic control, trajectory planning, carla leaderboard, simulation

## I. INTRODUCTION

### A. Motivation

Autonomous driving is a rapidly growing field that has the potential to revolutionize transportation by providing safer, more efficient, and convenient transportation for people around the world. One of the most critical aspects of autonomous driving is motion planning, which involves determining the optimal path for a vehicle to follow to reach its destination while avoiding obstacles and adhering to traffic rules. Motion planning is a complex task that requires sophisticated algorithms, advanced sensors, and powerful computing resources. Furthermore, with the rise of autonomous vehicles, there is a growing need for robust and reliable algorithms that can safely and efficiently navigate complex driving scenarios. One of the key challenges in developing such algorithms is the lack of a standardized evaluation platform that can be used to compare the performance of different algorithms. The CARLA (Car Learning to Act) Leaderboard Challenge [29] is an open competition designed to address this challenge by providing a common platform for evaluating the performance of autonomous driving algorithms. The challenge is based on the CARLA simulator [30], an open-source software platform that enables researchers and developers to test and develop their algorithms in a safe and controlled environment. In

this paper, our main focus is about the motion planning stage in autonomous driving (see Section II). Moreover, we briefly introduce our approaches applied in CADL in Section III. Finally, the evaluation of our result on CADL challenge compared to other competitors will be shown in Section IV.

### B. Related work

Motion planning is a crucial component of autonomous driving that involves generating a safe trajectory or path for the vehicle to follow in order to navigate through the environment. Many existing methods have been proposed to address this task, each with its own strengths and limitations.

Sampling-based methods randomly sample the environment and attempt to connect the samples, based on agent kinematics, to create a path, known as probabilistic sampling-based algorithms. Examples of these methods include Rapidly-exploring Random Trees (RRT) [1], [2] and Probabilistic Roadmaps (PRM) [3], [4]. Although the best path produced by these algorithms is often far from optimal, in [5], the authors proposed the Rapidly-exploring Random Graphs (RRG) algorithm to ensure the returned solution is asymptotically optimal. The authors introduced RRT\*, which is based on RRG to constructs a tree from an existing graph, while also improving the cost-to-come value of the neighbor vertices for sampling points [6]. Although these methods are computationally efficient and can handle unknown environments, their performance suffers from random distribution, making them insufficient to apply in well-defined environments, such as urban or highway driving. To take advantage of structured environments, lattice planners are introduced in reactive motion planning. These methods produce a finite set of trajectories that sample over the spatio-temporal evolution space, satisfying agent kinematics, dynamics, and environmental constraints, such as obstacles, lane markings, and traffic signals. In [7], [8], the authors decouple lateral and longitudinal movements to generate dynamics profile under Frenét frame to generate a set of trajectories, defined according to the driving state of the agent. Following the generation of the trajectory set, obstacle representation is a crucial aspect of ensuring safe and efficient navigation. Obstacle representations, such as circular [9], triangular [10], rectangular [11], are proposed to improve coverage and computational efficiency.

Optimization-based methods use optimization techniques to find the optimal path that satisfies a set of constraints, such as minimum time or energy consumption. Model Predictive Control (MPC) [11], [14], [15] and Differential Dynamic

Programming [16], [17] are examples of optimization-based methods. In urban driving scenarios, the automated vehicle needs to solve a joint optimization of neighboring vehicles (NV) costs over a receding horizon. To handle such task, a mixed integer quadratic programming (MIQP) formulation of the MPC is presented in [12] to handle the multi-input multi-output (MIMO) control problem with indicator variables and disjunctive constraint. MIQP is formulated to express OR logic for collision avoidance, combined with vehicle-to-everything (V2X) connectivity and MPC module to generate optimal trajectory. Base from this idea, [13] suggests adaptive interactive mixed integer MPC (aiMPC), which captures dynamics and collision avoidance constraints to predict the trajectory of the ego and NV in MPC horizon.

AI-based methods are another category of motion planning algorithms that use machine learning, deep learning or reinforcement learning algorithms to learn mappings between the current state of the vehicle, sensors, environments, and the optimal action to take, namely end-to-end autonomous driving. These methods can handle complex and dynamic environments, but they require large amounts of data and time to train. [18] vectorizes the sensors' information with multiple modalities, such as OpenDRIVE HD Map, Radar, LiDAR, front camera image, into same sized inputs. With different sensor domains, CNN-based fusion layers, or Transformer-based one [19], [23], [26], are proposed to offer a chance for these sensor data to find relations with each other. [20], [22] offer deep reinforcement learning (DRL) techniques that learn state-action policies from offline replay buffer (RB) (recorded from expert data) and online exploration agent from online RB.

## II. MOTION PLANNING METHOD

In this section, the reactive motion planning task is formulated in Frenét frame by the decouple of lateral and longitudinal movements to generate dynamics profiles for the agent. Furthermore, the constraints in urban driving scenarios are explained in details.

### A. Trajectory Planning in Frenét Frame

The work in this section is based on the proposal of using Frenét Frame method in [7]. Following this paper, we generate the trajectory sets using multiple terminal conditions to follow the center lines on the road (reference lines), then the conversion from Frenét frame to Cartesian frame is performed to spatio-temporal collision checking with other surrounding agents. As the most advantage of using Frenét frame in trajectory generation stage is that the reference lines are standardized in the same form of straight line with the difference in road boundaries. Nevertheless, the side effects of the usage of this method are mentioned in [32]. To avoid those disadvantages, the sampling of trajectory set is executed in Frenét frame using simplified kinematic model and driving comfort constraints, then the valid set is evaluated with environment constraints (detailed in II-B) in Cartesian space.

The Frenét frame is composed of tangential and normal vector to model the reference curve in Cartesian coordinate. In motion planning using Frenét frame, the tracking problem is composed of two factors: lateral and longitudinal offset along temporal dimension, namely  $d(t)$  and  $s(t)$  respectively. The movement profiles of our agent are defined in lateral direction  $D = [d(t), \dot{d}(t), \ddot{d}(t), \overset{\cdot\cdot\cdot}{d}(t)]$  and longitudinal one  $S = [s(t), \dot{s}(t), \ddot{s}(t), \overset{\cdot\cdot\cdot}{s}(t)]$ . As the decouple of lateral and longitudinal space, we use quintic polynomials for  $d(t)$  and  $s(t)$  within time interval  $T$ .

The generated trajectory needs to satisfy the jerk-optimal constraints. Therefore, the total jerk is accumulated of jerk in planning horizon, applied in both lateral jerk polynomial  $\overset{\cdot\cdot\cdot}{s}(t)$  and longitudinal jerk  $\overset{\cdot\cdot\cdot}{d}(t)$

$$J_s = \int_0^T \overset{\cdot\cdot\cdot}{s}{}^2(t) dt$$

$$J_d = \int_0^T \overset{\cdot\cdot\cdot}{d}{}^2(t) dt$$

Furthermore, to satisfy the comfort movement, the trajectory must obey the conditions that

$$\overset{\cdot\cdot\cdot}{s}(t) < J_{max}, \overset{\cdot\cdot\cdot}{d}(t) < J_{max}, \forall t \in [0, T]$$

where  $J_{max}$  is the maximum comfort jerk.

In urban driving, many modes are selected and executed while travelling to ensure the continuity of movement. These modes, in descending order of aggressiveness, are merging, following, velocity-keeping in free space, stopping. The behavior layer evaluates the consequences of mentioned modes to make decision. In the scope of this paper, we use solely the total cost functional to select the most optimal trajectory and the driving style of our agent is configurable by parameters regarding these functions.

Each mode has two cost functions related to lateral and longitudinal space in Frenét frame. The start condition is the current state of ego agent, which is retrieved from sensors (explained in III-A). The longitudinal and lateral terminal condition is given on selected mode, namely  $S$ ,  $D$ . The evaluation of trajectory corresponding to terminal condition is formulated by cost function  $C$ .

We define the common terminal state and cost function for longitudinal trajectory generation as

$$S_{ij} = [s_j, \dot{s}_j, \ddot{s}_j, T_i] \quad (1)$$

$$C_s = k_j J_s + k_t T_i + k_s (s_d - s_j)^2 \quad (2)$$

with  $s_d$  is the target distance in longitudinal frame.

In the stopping mode, the agent has to stop its movements before the longitudinal position of the traffic sign (or red light), which is  $(s_d)$ . Following (1), the terminal condition with the different  $\Delta s_j$  is

$$S_{ij} = [s_j, \dot{s}_j, \ddot{s}_j, T_i] = [s_d - \Delta s_j, 0, 0, T_i]$$

In following mode, or cruise control, we maintain the safe distance with the preceding vehicle. The state corresponding

to the preceding vehicle  $S_{pv} = [s_{pv}(t), \dot{s}_{pv}(t), \ddot{s}_{pv}(t)]$ . We define the predicted terminal state of the target vehicle in the prediction horizon as  $\hat{S}_{pv}(T) = [\hat{s}_{pv}(T), \dot{\hat{s}}_{pv}(T), \ddot{\hat{s}}_{pv}(T)]$ , which is retrieved from the Trajectory Prediction module (detailed in III-C). Using (1), the desired states of our agent are as follows

$$\begin{aligned} s_j &= \hat{s}_{pv}(T) - [D_0 + \tau \dot{\hat{s}}_{pv}(T)] \\ \dot{s}_j &= \dot{\hat{s}}_{pv}(T) \pm \Delta \dot{s}_j - \tau \ddot{\hat{s}}_{pv}(T) \\ \ddot{s}_j &= \ddot{\hat{s}}_{pv}(T) \end{aligned}$$

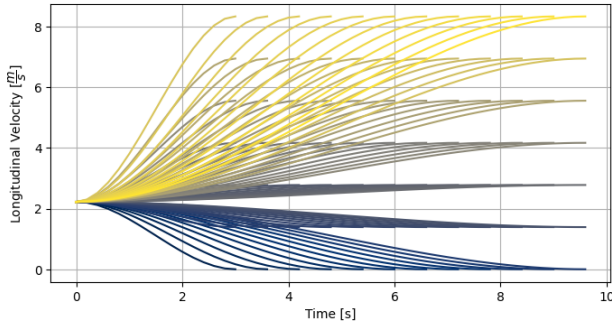
with  $D_0$  is the constant safety distance with the other agent, following by the gap defined by constant time-to-collision  $\tau$ .

In merging mode, it requires the agent to keep appropriate distance to both preceding and following vehicles. Using the predicted trajectories of preceding  $\hat{S}_{pv}(t)$  and following  $\hat{S}_{fv}(t)$  vehicles, we can define the target point in the terminal condition (1)

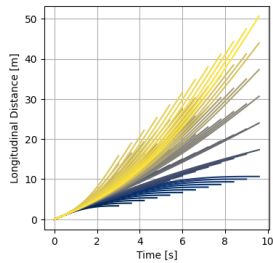
$$s_j = \frac{1}{2} [\hat{s}_{pv}(T) + \hat{s}_{fv}(T)],$$

Corresponding to velocity-keeping mode, we keep our agent to maintain its velocity without specific  $s_d$ . As shown in Fig. 1, we use quartic polynomials for the generation of  $s(t)$ . The terminal state is formulated as follows, where  $\dot{s}_d$  is the desired velocity.

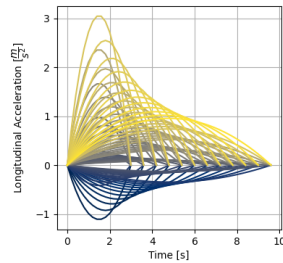
$$\begin{aligned} S_{ij} &= [\dot{s}_d \pm \Delta \dot{s}_j, 0, T_i] \\ C_v &= k_j J_s + k_t T_i + k_s (\dot{s}_d - \dot{s}_j)^2 \end{aligned}$$



(a) Longitudinal velocity



(b) Longitudinal distance

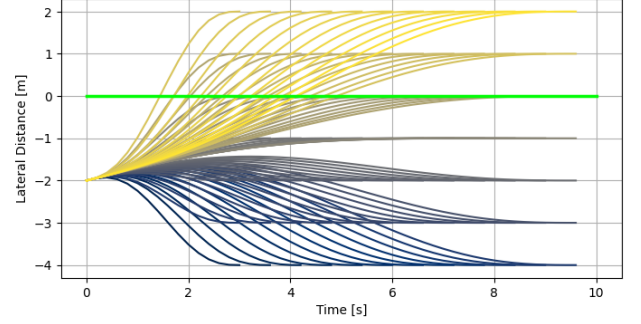


(c) Longitudinal acceleration

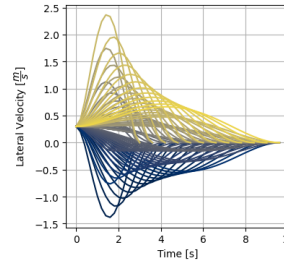
Fig. 1. The longitudinal profile based on velocity tracking is shown as: (a) longitudinal velocity, (b) longitudinal distance, (c) longitudinal acceleration. Each solution is color-mapped by its longitudinal target velocity  $s_j$ .

Regarding lateral space, we generate the trajectory set in lateral space with multiple offset  $d_j$  (with the difference  $\Delta d$ ) and time interval  $T_i$  in terminal condition. The ultimate state is that our agent successfully tracks the reference line ( $d_T = 0$ ). Similar to longitudinal space, the terminal condition is defined as

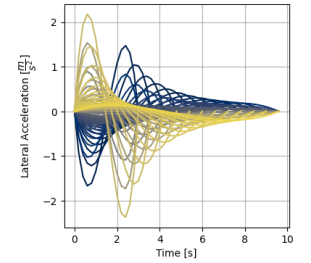
$$\begin{aligned} D_{ij} &= [d_j, 0, 0, T_i] \\ C_d &= k_j J_d + k_t T_i + k_s d_j^2 \end{aligned}$$



(a) Lateral movement



(b) Lateral velocity



(c) Lateral acceleration

Fig. 2. The illustrations of lateral movement (a), its corresponding velocity (b) and acceleration (c) in Frenét frame. The green line is the target lateral offset with reference line (at zero). Multiple solutions in (a) are generated with the lateral and time interval difference,  $\Delta d = 1m$  and  $\Delta T = 0.6s$  respectively, color-mapped by its lateral offset  $d_j$ .

## B. Environment Constraints

In our urban driving task, the constraints include collision boundary of NV and pedestrians, road barriers, traffic lights and road signs. In this stage, our trajectories in Frenét frame are converted into the ones in Cartesian space, denoted by  $[x(t), y(t), \theta(t), v(t), a(t)]$ , where  $[x(t), y(t)]$  is the position,  $\theta(t)$  is the orientation angle,  $v(t)$  is the velocity and  $a(t)$  is the acceleration of trajectory points with respect to (w.r.t) our ego agent.

To improve the computation effort, we use different representation for vehicles (including our ego agent): three-disk or five-disk methods to cover the rectangular shape of the NV. As illustrated in Fig. 3, there are two types of disk representation that being used for collision checking: three-disk and five-disk models. While both models are able to cover the whole rectangular section, there is a trade-off between computational efficiency by using the three-disk model and precise representation by using the second model, which has

smaller combined coverage. With mentioned advantage, we will use the three-disk model with same size for vehicle representation, which could be constructed by 2D center point and radius as  $D = [x, y, r]$  in the relative coordinate of vehicle

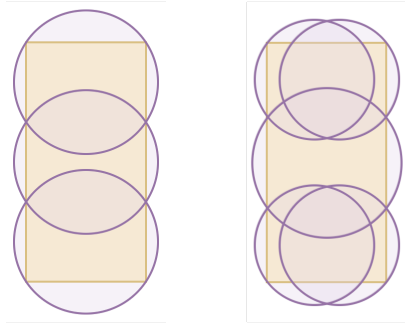
$$\begin{aligned} D_1 &= [0, 0, R_{max}] \\ D_2 &= \left[ \frac{l}{3}, 0, R_{max} \right] \\ D_3 &= \left[ -\frac{l}{3}, 0, R_{max} \right] \end{aligned}$$

where  $D_1, D_2, D_3$  are the models of three disks in center, front and back respectively.  $w$  is width,  $l$  is length of the vehicle, and  $R_{max} = \left( \frac{w^2}{4} + \frac{l^2}{36} \right)$ .

The collision is violated when

$$\|p_{ego}^i - p_{nv}^j\| < R_{max}, i, j = 1, \dots, 3.$$

with  $p_{ego}^i$  is the center location of  $i$ th disk of ego vehicle and  $p_{nv}^j$  is the center location of  $j$ th disk of NV.



(a) Three-disk model (b) Five-disk model

Fig. 3. Disk representation (purple) of the rectangular vehicle (orange). By using more disks, the rectangular could be represented more precise. However, there will be computational overhead in the collision checking process.

In CARLA simulation, the road boundaries, traffic lights and road signs' positions can be retrieved from the provided map. However, the state of traffic light (green, yellow, red) can only be identified visually by camera (by methods explained in III-B). We convert the queried positions on the global frame and their states into terminal conditions in motion planning, as described in the previous section.

### III. CARLA LEADERBOARD APPROACH

In CADL, there are two tracks to submit the solution, namely SENSORS and MAPS tracks. In SENSORS, the set of sensors provided includes GNSS, IMU, LiDAR, RADAR, RGB camera (limit to 4 units), Speedometer. Similarly, the MAPS track provides the same set with additional OpenDRIVE map. Our approach is tested and submitted on MAPS track. In this section, because of the limited scope of this paper, we briefly introduce the methods, without digging into details, that we use to handle the sensor signals. Fig. 4 shows a scenario in CADL from the bird-eye view, including the

output of three modules: localization, perception and trajectory prediction.

#### A. Localization

To retrieve a precise position of ego vehicle using GNSS information (latitude  $\lambda$ , longitude  $\phi$ , altitude  $\varphi$ ), IMU (angular velocity  $[va_x, va_y, va_z]$ , linear acceleration  $[al_x, al_y, al_z]$ , yaw compass  $\psi$ ), the many methods to fuse aforementioned data and estimate the ego current state are proposed using Kalman Filtering (KF) [34] list more. The simplified formulation to produce estimated ego state is

$$[\hat{x}, \hat{y}, \hat{\theta}, \hat{v}, \hat{a}] = \text{KF}(\lambda, \phi, va_x, va_y, al_x, al_y, \psi)$$

#### B. Perception

Regarding the detection of surrounding vehicles, pedestrians, we use the point cloud data  $PC$  from LiDAR sensor. We apply a pre-trained model from [35] to predict the bounding boxes of surrounding vehicles and pedestrians, called moving obstacles. The prediction has output of object 3D shape  $[h_{mo}, w_{mo}, l_{mo}]$ , 3D position  $[x_{mo}, y_{mo}, z_{mo}]$ , yaw angle  $\psi_{mo}$ , and the detection confidence. Subsequently, we apply the KF to predict velocity  $v_{mo}$ , acceleration  $a_{mo}$  of the moving obstacles. The state that describe a moving obstacle

$$S_{mo} = [x_{mo}, y_{mo}, \psi_{mo}, v_{mo}, a_{mo}]$$

On the other hand, the detection and recognition of traffic light, traffic sign is executed following the detection model of [36]. Firstly, we collect the training images from our test run in Carla simulator. Secondly, we re-train the model using the approach of transfer learning. Eventually, with the output of the trained model (2D location  $[x_{im}, y_{im}]$  on image, recognition of traffic light state, traffic sign), we combine these with the landmarks provided in the OpenDRIVE map, to get its state and location relative to ego agent.

#### C. Trajectory Prediction

Based on the dynamic state of the moving obstacle  $S_{mo}$  and OpenDRIVE map given in CARLA simulator, we predict its future trajectory in the planning horizon.

The original map topology contains the tuple of pairs of waypoints located either at the point a road begins or ends. The first element of a pair is the origin and the second one represents another road end that can be reached. Because each road has different length, we create a dense graph to represent the given topology with fixed sampling distance. An R-Tree is additionally used for graph index querying in spatial dimension.

Firstly, we assume that other vehicles in simulation strictly follow the road center without any deviation. With the vehicle's position, the corresponding node in the dense graph is queried using R-Tree indexing. Then, the Breadth-First Search algorithm is applied on the dense graph to extract the possible paths that have their length closed to a desired distance. Finally, spatio-temporal trajectories are generated using the Pure Pursuit algorithm, based on the feasible paths.

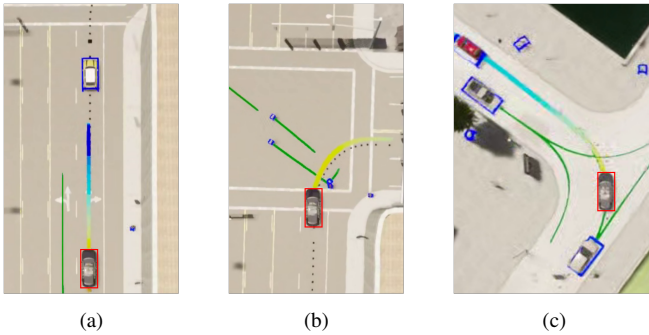


Fig. 4. Our agent (red box) maneuvers on the street in CADL. Its position relative to the map is constructed by the Localization module. The moving obstacles within the field of view of LiDAR (including vehicles and pedestrians) are detected by Perception module and bounded with blue boxes. The predicted trajectories of obstacles are shown by green lines. Our agent follows the trajectory generated by the motion planning module, which is color-mapped by corresponding velocity (blue: stopping speed, orange: low speed, red: high speed). The reference path is displayed in a black dot line. In the illustrations, these shows the scenarios: (a) stopping and keeping safe distance with preceding vehicle (b) section crossing through lots of pedestrians (c) crossing the three-way section.

## IV. RESULT AND DISCUSSION

### A. Metrics

In the CADL challenge, a set of metrics is provided to describe the driving proficiency of an agent. The main metrics are as follows

- **Route completion** is the percentage of the route distance completed by an agent. The evaluation stops for each scenario when the violation occurs, such as collision and agent being blocked for the specific interval (180 seconds).
- **Infraction penalty** is the metric is used to show how safety the driving is. The value will decay for each time the agent commits a violation, based on the corresponding ratio. This metric value is in the range of  $[0, 1]$
- **Driving score** is the main metric of the CADL, which is used to rank between the participants. It is the product between the route completion ratio and the infraction score. Unit is %.

There are many types of infractions in CADL, including Collisions with pedestrians, Collisions with vehicles, Collisions with layout, Running a red light, Route deviation, Agent blocked. Each type comes with a specific penalty coefficient that affects the total score of the Infraction penalty.

### B. Evaluation / Result on CADL

As in table I, we compare our method with other participants in the MAPS track of the CADL challenge [30]. Our PaaS ranks third on the leaderboard, with the driving score of 48.24. Nevertheless, our approach achieves the highest infraction penalty 0.84, proving that the agent is able to drive safely throughout the test set given in CADL challenge. Looking into the details of infractions, we can tell that our agent could avoid

the violation with surrounding agents, static environment, running red light, and route deviations.

However, the figure of pedestrian collisions is higher than the two participants in first and second rank. The detection of pedestrians using LiDAR is not effective, due to the fact that human size is small compared to the resolution of the sensor. Secondly, predicted trajectories of pedestrians are not matching with the actual human behavior in CADL. Moreover, there are such cases in CADL that the pedestrian suddenly crosses the road from the blind view of our agent, and we could not react well enough to that behavior.

As we mention in II-A, we rely solely on cost function of trajectory to select the most optimal path. In some specific scenarios, choosing the trajectory with the lowest cost does not always result in the most optimal solution, especially in dense traffic. Therefore, our figure of agent blocked is unusually high compared to the rest of participants.

## V. CONCLUSION AND FUTURE WORKS

In this paper, we propose the trajectory planning for autonomous driving in urban environment and our solutions to conquer the CADL challenge. The trajectory generator produces a reliable and safety maneuver over the planning horizon. However, in several complex cases, the planner is not able to compose an optimal path regarding the semantic understanding of the surroundings due to the fact that the parameters of cost function are fixed during different scenarios.

To solve this circumstance, adaptive cost functions could be added to the current approach, which requires extensive review of the scenarios in the challenge. Furthermore, adding a behavior layer would fill the gap in the decision-making problem in our current approach. By applying the partially observable Markov decision process and its alternatives, we can further increase the reasoning capability of our agent.

## REFERENCES

- [1] J. J. Kuffner, S. Kagami, K. Nishiwaki, M. Inaba, and H. Inoue, "Dynamically-Stable Motion Planning for Humanoid Robots," *Autonomous Robots*, vol. 12, no. 1, pp. 105–118, Jan. 2002.
- [2] J. J. Kuffner and S. M. LaValle, "RRT-connect: An efficient approach to single-query path planning," in *Proceedings 2000 ICRA. Millennium Conference. IEEE International Conference on Robotics and Automation. Symposia Proceedings (Cat. No.00CH37065)*, Apr. 2000, pp. 995–1001 vol.2.
- [3] L. E. Kavraki, M. N. Kolountzakis, and J.-C. Latombe, "Analysis of probabilistic roadmaps for path planning," *IEEE Transactions on Robotics and Automation*, vol. 14, no. 1, pp. 166–171, Feb. 1998.
- [4] L. E. Kavraki, P. Svestka, J.-C. Latombe, and M. H. Overmars, "Probabilistic roadmaps for path planning in high-dimensional configuration spaces," *IEEE Transactions on Robotics and Automation*, vol. 12, no. 4, pp. 566–580, Aug. 1996.
- [5] S. Karaman and E. Frazzoli, "Sampling-based motion planning with deterministic  $\mu$ -calculus specifications," in *Proceedings of the 48th IEEE Conference on Decision and Control (CDC) held jointly with 2009 28th Chinese Control Conference*, Dec. 2009, pp. 2222–2229.
- [6] S. Karaman and E. Frazzoli, "Sampling-based algorithms for optimal motion planning," *The International Journal of Robotics Research*, vol. 30, no. 7, pp. 846–894, Jun. 2011.
- [7] M. Werling, J. Ziegler, S. Kammel, and S. Thrun, "Optimal Trajectory Generation for Dynamic Street Scenarios in a Frenet Frame," presented at the *Proceedings - IEEE International Conference on Robotics and Automation*, Jun. 2010, pp. 987–993.

TABLE I  
TEST-SET EVALUATION RESULT ON CARLA LEADERBOARD CHALLENGE

Rank	Name	Driving score	Route compl.	Infrac. penalty	Collision pedes.	Collision vehicle	Collision layout	Red light infrac.	Route deviations	Agent blocked
		%, ↑	%, ↑	[0, 1], ↑	#/km, ↓	#/km, ↓	#/km, ↓	#/km, ↓	#/km, ↓	#/km, ↓
1	Map TF++	<b>61.17</b>	81.81	0.70	<b>0.01</b>	0.99	0.00	<b>0.08</b>	0.00	0.55
2	MMFN+ [18]	59.85	<b>82.81</b>	0.71	0.01	0.59	0.00	0.51	0.00	<b>0.06</b>
3	<b>PaaS (ours)</b>	48.24	60.68	<b>0.84</b>	0.10	<b>0.23</b>	<b>0.00</b>	0.13	<b>0.00</b>	4.13
4	GRI-based DRL [20]	33.78	57.44	0.57	0.00	3.36	0.50	0.52	1.47	0.80
5	MMFN [18]	22.80	47.22	0.63	0.09	0.67	0.05	1.07	0.00	1003.88
6	Techs4AgeCar+	18.75	75.11	0.28	1.52	2.37	1.27	1.22	0.17	1.28
7	Pylot	16.70	48.63	0.50	1.18	0.79	0.01	0.95	0.44	3.30
8	CaRINA [33]	15.55	40.63	0.47	1.06	3.35	1.79	0.28	0.34	7.26
9	Techs4AgeCar	12.63	61.59	0.33	2.25	0.63	0.00	0.96	0.02	1.34

↑ : Higher is better.      ↓ : Lower is better.      #/km : number of infractions per kilometer.

- [8] M. Werling, S. Kammel, J. Ziegler, and L. Gröll, "Optimal trajectories for time-critical street scenarios using discretized terminal manifolds," *The International Journal of Robotics Research*, vol. 31, no. 3, pp. 346–359, Mar. 2012.
- [9] H. Mouhagir, R. Talj, V. Cherfaoui, F. Aioun, and F. Guillemard, "Integrating safety distances with trajectory planning by modifying the occupancy grid for autonomous vehicle navigation," in *2016 IEEE 19th International Conference on Intelligent Transportation Systems (ITSC)*, Nov. 2016, pp. 1114–1119.
- [10] J. Nilsson, J. Fredriksson, and E. Coelingh, "Trajectory planning with miscellaneous safety critical zones \*\*This work was supported by FFI - Strategic Vehicle Research and Innovation.," *IFAC-PapersOnLine*, vol. 50, no. 1, Elsevier BV, pp. 9083–9088, Jul. 2017.
- [11] X. Yang and H. Li, "Model Predictive Motion Planning for Autonomous Vehicle in Mid-high Overtaking Scene," *2020 IEEE 91st Vehicular Technology Conference (VTC2020-Spring)*, pp. 1–5, May 2020.
- [12] R. A. Dollar and A. Vahidi, "Predictively Coordinated Vehicle Acceleration and Lane Selection Using Mixed Integer Programming," *ASME 2018 Dynamic Systems and Control Conference, American Society of Mechanical Engineers Digital Collection*, Nov. 2018.
- [13] V. Bhattacharyya and A. Vahidi, "Automated Vehicle Highway Merging: Motion Planning via Adaptive Interactive Mixed-Integer MPC," unpublished, 2022.
- [14] H. Wang, Y. Huang, A. Khajepour, Y. Zhang, Y. Rasekhipour, and D. Cao, "Crash Mitigation in Motion Planning for Autonomous Vehicles," *IEEE Transactions on Intelligent Transportation Systems*, vol. 20, no. 9, pp. 3313–3323, Sep. 2019.
- [15] S. Dixit et al., "Trajectory Planning for Autonomous High-Speed Overtaking in Structured Environments Using Robust MPC," *IEEE Transactions on Intelligent Transportation Systems*, vol. 21, no. 6, pp. 2310–2323, Jun. 2020.
- [16] J. van den Berg, S. Patil, and R. Alterovitz, "Motion Planning Under Uncertainty Using Differential Dynamic Programming in Belief Space," in *Robotics Research: The 15th International Symposium ISRR*, H. I. Christensen and O. Khatib, Eds., in *Springer Tracts in Advanced Robotics*. Cham: Springer International Publishing, 2017, pp. 473–490.
- [17] H. Li and P. M. Wensing, "Hybrid Systems Differential Dynamic Programming for Whole-Body Motion Planning of Legged Robots," *IEEE Robot. Autom. Lett.*, vol. 5, no. 4, pp. 5448–5455, Oct. 2020.
- [18] Q. Zhang, M. Tang, R. Geng, F. Chen, R. Xin, and L. Wang, "MMFN: Multi-Modal-Fusion-Net for End-to-End Driving," *IEEE/RSJ International Conference on Intelligent Robots and Systems (IROS)*, Oct. 2022, pp. 8638–8643.
- [19] A. Prakash, K. Chitta, and A. Geiger, "Multi-Modal Fusion Transformer for End-to-End Autonomous Driving," *2021 IEEE/CVF Conference on Computer Vision and Pattern Recognition (CVPR)*, pp. 7073–7083, Jun. 2021.
- [20] R. Chekroun, M. Toromanoff, S. Hornauer, and F. Moutarde, "GRI: General Reinforced Imitation and its Application to Vision-Based Autonomous Driving," *Conference on Neural Information Processing Systems (NeurIPS) 2021, Machine Learning for Autonomous Driving Workshop*, Dec 2021.
- [21] M. Toromanoff, E. Wirbel, and F. Moutarde, "End-to-End Model-Free Reinforcement Learning for Urban Driving Using Implicit Affordances," *2020 IEEE/CVF Conference on Computer Vision and Pattern Recognition (CVPR)*, IEEE, Jun. 2020.
- [22] D. Chen, V. Koltun, and P. Krahenbuhl, "Learning to drive from a world on rails," *2021 IEEE/CVF International Conference on Computer Vision (ICCV)*, IEEE, Oct. 2021.
- [23] K. Chitta, A. Prakash, B. Jaeger, Z. Yu, K. Renz, and A. Geiger, "TransFuser: Imitation with Transformer-Based Sensor Fusion for Autonomous Driving," *Pattern Analysis and Machine Intelligence (PAMI)*, 2022.
- [24] D. Chen and P. Krahenbuhl, "Learning from All Vehicles," *2022 IEEE/CVF Conference on Computer Vision and Pattern Recognition (CVPR)*, IEEE, Jun. 2022.
- [25] P. Wu, X. Jia, L. Chen, J. Yan, H. Li, and Y. Qiao, "Trajectory-guided Control Prediction for End-to-end Autonomous Driving: A Simple yet Strong Baseline," *Conference on Neural Information Processing Systems (NeurIPS) 2022*, in press.
- [26] H. Shao, L. Wang, R. Chen, H. Li, and Y. Liu, "Safety-Enhanced Autonomous Driving Using Interpretable Sensor Fusion Transformer," *Conference on Robot Learning (CoRL)*, 2022.
- [27] Y. Zhang, J. Zhang, J. Zhang, J. Wang, K. Lu, and J. Hong, "A Novel Learning Framework for Sampling-Based Motion Planning in Autonomous Driving," in *Proceedings of the AAAI Conference on Artificial Intelligence*, Apr. 2020, pp. 1202–1209.
- [28] Y. Zhang, J. Zhang, J. Zhang, J. Wang, K. Lu, and J. Hong, "Integrating Algorithmic Sampling-Based Motion Planning with Learning in Autonomous Driving," *ACM Trans. Intell. Syst. Technol.*, vol. 13, no. 3, pp. 1–27, Jun. 2022.
- [29] C. Yu and S. Gao, "Reducing Collision Checking for Sampling-Based Motion Planning Using Graph Neural Networks," 2022, unpublished.
- [30] CARLA. Autonomous driving leaderboard. [Online]. Available: <https://leaderboard.carla.org/leaderboard>
- [31] A. Dosovitskiy, G. Ros, F. Codevilla, A. Lopez, and V. Koltun, "CARLA: An Open Urban Driving Simulator," *arXiv*, Nov. 10, 2017.
- [32] B. Li, Y. Ouyang, L. Li, and Y. Zhang, "Autonomous Driving on Curvy Roads Without Reliance on Frenet Frame: A Cartesian-Based Trajectory Planning Method," *IEEE Transactions on Intelligent Transportation Systems*, vol. 23, no. 9, pp. 15729–15741, Sep. 2022.
- [33] L. A. Rosero et al., "A Software Architecture for Autonomous Vehicles: Team LRM-B Entry in the First CARLA Autonomous Driving Challenge," 2020, unpublished.
- [34] J. H. Ryu, G. Gankhuyag, and K. T. Chong, "Navigation System Heading and Position Accuracy Improvement through GPS and INS Data Fusion," *Journal of Sensors*, vol. 2016, p. e7942963, Jan. 2016.
- [35] S. Shi et al., "PV-RCNN: Point-Voxel Feature Set Abstraction for 3D Object Detection," *2020 IEEE/CVF Conference on Computer Vision and Pattern Recognition (CVPR)*, Jun. 2020.
- [36] Z. Ge, S. Liu, F. Wang, Z. Li, and J. Sun, "YOLOX: Exceeding YOLO Series in 2021," Aug., 2021, unpublished.